Published by The College of Vocational and Technology Education (COVTED), TASUED, vol. 19, no 1, pp. 35-47.

COVTED, TASUED
The Vocational and Applied Science Journal (VAS)

Environmental Monitoring of Igbogila Lithology, North-Western, Ogun State using Radiometric Method

Ogunsanwo, F. O.
Department of Physics, Tai Solarin Federal University of Education, Ogun State, Nigeria
Corresponding email: *ogunsanwofo@tasued.edu.ng*

Abstract
This study investigates the environmental radiological implications and mineralogical signatures of the Igbogila lithology using ground radiometric data. The analysis focused on uranium (U), thorium (Th) and potassium (K) concentrations, their ratios (U/Th, U/K, Th/K), uranium migration index (UMI), and effective dose rate. The objectives were to assess uranium mobility, identify potential geochemical processes, and evaluate radiation exposure risks. The UMI spectra highlight spatial variability in uranium retention and leaching, with positive values indicating localized uranium enrichment and negative values reflecting strong leaching and thorium dominance. Notably, location A7 recorded the most negative UMI (≈ –14), which corresponded to the highest effective dose rate (> 2.0 mSv yr^{-1}), thereby suggesting thorium-controlled radiation hazards. In contrast, uranium-enriched zones exhibited relatively moderate dose rates (< 1.0 mSv yr^{-1}), implying that geochemical mobility of uranium does not always equate to elevated radiation exposure. The overall dose rates across the study area remained within international safety thresholds, though localized anomalies highlight potential environmental and health concerns. These results demonstrate that integrating UMI with dose-rate evaluation provides a robust approach to environmental monitoring and mineralogical assessment. The findings emphasize the dual need for groundwater monitoring in uranium-mobilized zones and radiation hazard management in thorium-rich terrains of the Igbogila area.

Keywords: Uranium migration index, Environmental radiological monitoring, Radioelement ratios; Effective dose rate

1. Introduction

Environmental monitoring of natural radioactivity in near-surface sediments is essential for assessing public health risks and the geochemical behavior of radioelements in continental settings (Olawale *et al.*, 2024; Makinde *et al.*, 2023). In sedimentary lithologies, the concentrations and spatial distributions of naturally occurring radioactive materials (NORM) such as principally uranium (U), thorium (Th) and potassium (K) has been found to always accompanied with primary provenance, diagenetic alteration and secondary mobility during weathering and groundwater flow (Uyanık 2022; Ogunsanwo *et al.*, 2025). These processes control radiogenic heat production, radon emanation potential, and the external gamma dose to which local populations and ecosystems may be exposed (Abu-Khader *et al.*, 2018). A focused radiometric assessment therefore serves dual purposes: (i) mapping geologic and geochemical heterogeneity for resource and hydrogeologic studies, and (ii) quantifying radiation exposure and environmental risk for regulatory and mitigation planning.

Human activities such as mining, milling and processing of uranium ores and mineral sands, manufacturing of fertilizers, burning fossil fuels, metal refining, among many others have been reported in literature to have great impact in the elevation of primordial natural radionuclides (U, Th and K) concentrations in the environment (Pujol and Sanchez-Cabeza 2000 ; Khattab *et al.*, 2021). Based on this, prior information about the geological processes and antrophological activities about any area to be understudied is needed for proper environmental monitoring and control of radioelements concentrations from time to time and climate to climate.

There are many controlling factors which enhance and attenuate the radioelement concentration such as precipitation, temperature, soil moisture, vegetation cover and many other (Uwah and Rosenberg, 1993; Ademila *et al.*, 2023). The geological formations and landslides also play a significant role in radiometric interpretation of the radioelements concentrations.

Surface and near-surface radiometric surveying (ground or airborne gamma-ray spectrometry) provides rapid, spatially continuous estimates of eU (equivalent uranium), eTh (equivalent thorium) and K (%), which when combined with laboratory analyses and soil sampling enable rigorous interpretation (Abuelnaga and Al-Garni, 2015; Okoro *et al.*, 2023; Bayoumi and Emad 2020). Beyond single-element concentrations, diagnostic indices and derived quantities are particularly informative for environmental monitoring. Elemental ratios such as U/Th, U/K and Th/K help distinguish between primary lithologic signatures and

Ogunsanwo F.O., (2025). Environmental Monitoring of Igbogila Lithology, North-Western, Ogun State using Radiometric Method. *The Vocational and Applied Science Journal (VAS)*, vol. 19, no. 1, pp. 35-47.

secondary processes. The elevated U/Th often signals uranium mobilization and redeposition while high U/K may indicate potassium depletion from alteration or enrichment of uranium. Th/K ratios generally trace felsic versus mafic provenance and degree of crustal evolution (Abdel-Hakeem *et al.,* 2023). These ratios, interpreted alongside geological mapping, reveal the relative roles of provenance, diagenesis and weathering in controlling radioelement distribution within the Igbogila sediments.

The Uranium Migration Index (UMI) synthesizes elements of mobility and redistribution. High UMI signals intensive alteration and U mobility (with implications for groundwater contamination and secondary uranium deposits), whereas low UMI implies uranium retention in primary mineral hosts and a steadier contribution to radiogenic heat (Asfahani *et al.,* 2007; Hennig and Kühn, 2021; Akingboye *et al.,* 2022; Altundaş and Çınar, 2023).Because uranium mobility links geochemistry to hydrogeology, UMI maps are particularly informative for assessing both resource potential and environmental vulnerability.

From the public-health perspective, estimated effective dose rate is the bridge between geoscience and risk assessment (Ademoroti, *et al.,* 2024; Eke *et al*., 2024; Mbonu *et al*., 2025). External gamma exposure (derived from surface U, Th, K concentrations) is the principal short-term pathway for population exposure on land. However, inhalation of radon and its decay products mobilized from U-bearing materials into built environments can present greater long-term health risk (Abu-Khader *et al.,* 2018; Elegbede *et al.,* 2025). Thus, radiometric monitoring should be coupled with radon surveys, groundwater assays, and soil/food chain sampling where anomalies are found.

Despite the environmental and economic importance, few studies have systematically integrated spatial radiometric mapping, radioelement ratios, dose-rate modeling and UMI assessment for sedimentary successions in southwestern Nigeria. The Igbogila sediments, with variable grain size, organic content and weathering profiles, provide an ideal strategy to evaluate how sedimentary facies, permeability contrasts and surface processes modulate radioelement behavior and exposure risk. Such integrated monitoring is also timely for local land-use planning: agricultural practices, groundwater abstraction, and building construction can all be informed by spatially resolved radiometric and dose data.

This study therefore applies ground radiometric surveying and targeted soil sampling across the Igbogila sedimentary lithology to (i) map eU, eTh and K distributions, (ii) compute and interpret radioelement ratios (U/Th, U/K, Th/K) and the, (iii) derive spatial effective dose-rate and Uranium Migration Index maps, and (iv) assess environmental and public-health implications within a geological framework. By linking geochemical indices with radiological metrics, the work aims to provide actionable data for both resource evaluation and environmental management in the Igbogila area.

2. Materials and Methods

2.1 Sample Collection and Laboratory Analysis

In this study twenty (20) soil samples were collected randomly across Igbogila, North-eastern Nigeria. In Figure 1, the locations of Igbogila in which samples were collected have been shown. Soil samples were collected to a depth of 7-9 cm using a coring tool that was thoroughly cleaned and dried before each sample was collected. A reference soil sample was included in each set of analysis to check the precision of the analysis in the laboratory. At least two replicates were carried out for all analyses. Laboratory analyses were conducted at Radiation and Health Physics Research Laboratory, Department of Physics, Federal University of Agriculture, Abeokuta (FUNAAB). The sample locations were recorded in term of its latitudinal and longitudinal using a hand held Global Positioning System (GPS) – Garmin model.

Ultimate care was taken in the extraction of soil sections to avoid mixing or cross contamination of soil samples. Approximately 2 kg of each sample were collected in a plastic bag at the sampling points. The soil samples were processed according to the procedure recommended by the International Atomic Energy Agency (2003). Soil samples were well mixed after removing exotic materials such as pieces of stones and gravel. The samples were weighed and then dried in an oven at 110˚C. After shaking thoroughly, the samples were sieved with a 1 mm mesh screen (Faweya and Babalola, 2010). The samples were dried, sieved, packed in 1L Marinelli beaker and sealed for 4 weeks to reach secular equilibrium between 226Ra (daughter of 238U) and 232Th with their daughter nuclei. This was done to allow radon and its short-lived progenies to reach secular radioactive equilibrium prior to gamma spectroscopy (Dabayneh *et al.,* 2010).The radioelement concentration for K, eTh and eU was recorded in Becquerel per Kilogram (Bq/kg).

2.2 Conversion from Becquerel per kilogram (Bq/kg) to part per million (ppm) and percent (%)

The radioelement concentrations were converted from Bq/kg to ppm and % using conversion factor as given by Polish Central Laboratory for Radiological Protection (Ogunsanwo *et al.,* 2023; Malczewski *et al.,* 2004) as shown in Equations 1 to 3 for uranium in ppm, thorium in ppm and potassium respectively.

$$C_U(ppm) = C_U(Bq/kg) \times 0.08045 \quad (1)$$

$$C_{Th}(ppm) = C_{Th}(Bq/kg) \times 0.24331 \quad (2)$$

$$C_K(ppm) = C_K(Bq/kg) \times 0.003296 \quad (3)$$

where C_U, C_{Th} and C_K are the concentration of ^{238}U,

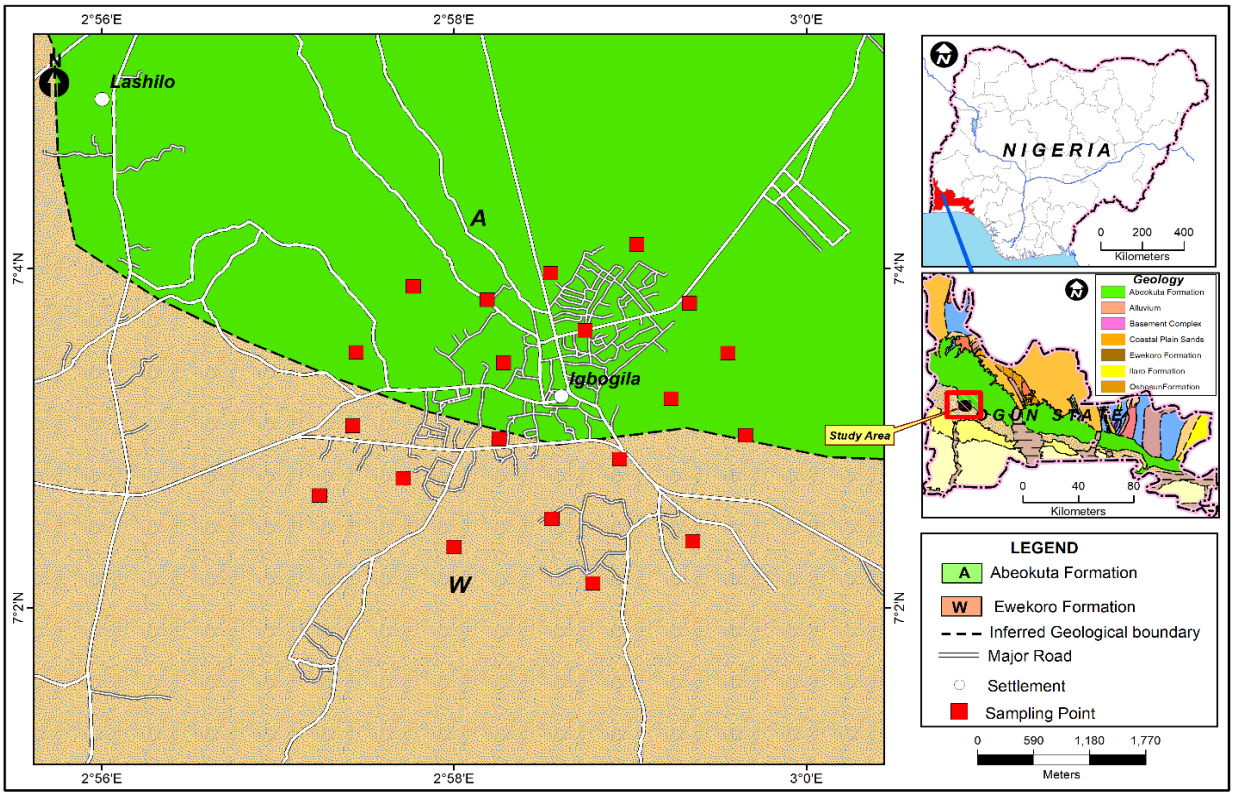

Figure 1: Map of study area showing the sampling station

^{232}Th and ^{40}K respectively.

The radiometric data are then later summarized in terms of color images obtained from minimum curvature grids in order to avoid image colour bias and to enhance the signal to noise ratio. Results of the gamma-ray measurements are displayed as concentration maps for eU, eTh, K, equivalent dose and uranium migration index image. In addition, ratio maps (eU/eTh, eU/K, eTh/K) maps are also generated. Generally, the maps are depicted as high - moderate-low radioactive concentrations across the whole area. It is evident from the various maps produced that there are soils/rocks with different concentrations of the natural radioelements.

2.3 Radioelement Ratios in Environmental Assessment

The ratios U/Th, U/K, and Th/K are vital tools for detecting geochemical processes in the environment. U/Th ratio is used to investigate uranium enrichment due to mobilization and secondary deposition (anomalously high values), often linked to water–rock interaction, weathering, or anthropogenic activities (mining and waste disposal). U/K ratio is majorly used to highlights uranium migration relative to K-rich minerals (El-Qassas, 2020). It is also useful in identifying altered or leached zones and distinguishing natural background from anomalous enrichment. Th/K ratio acts as a lithological discriminator. Significant deviations may indicate changes in soil composition, weathering intensity, or enrichment in resistant Th-minerals. The radioelement ratios assessment across gives detailed information and insight that can monitor zones of uranium mobilization, environmental alteration, geothermal and potential contamination hotspots.

2.4 Environmental Risk Assessment

In this study, the risk associated with the study area are assessed by computing two radioactive related parameters, namely; exposure and dose rate, and uranium migration index.

2.5 Exposure and dose rate Estimation

The exposure and dose rate estimation combined radiation contribution from U, Th, and K over the lithological unit. Monitoring dose rate is crucial for investigating the baseline studies, risk assessment, environmental safety by ensuring radiation exposure levels remain below international safety limits and pose no long-term health risks. (ICRP; 1994; IAEA, 2003; UNSCEAR, 2000).A high dose rate may reflect uranium- or thorium-rich soils, granitic terrains, or anthropogenic input from mining residues.

In order to verify the environmental effects due to these natural radiometric concentrations, the exposure rates, E (μR/hr), and the equivalent dose rates, D(mSv/yr), were calculated using the following equations, respectively (Abuelnaga and Al-Garni, 2015; Olowofela et al., 2019):

$$E(\mu R/hr) = 1.505K(\%) + 0.287eTh(ppm) + 0.653eU(ppm) \quad (4)$$

$$D(mSv/yr) = 0.0833 \times E(\mu R/hr) \quad (5)$$

where, eTh, eU and K are the equivalent

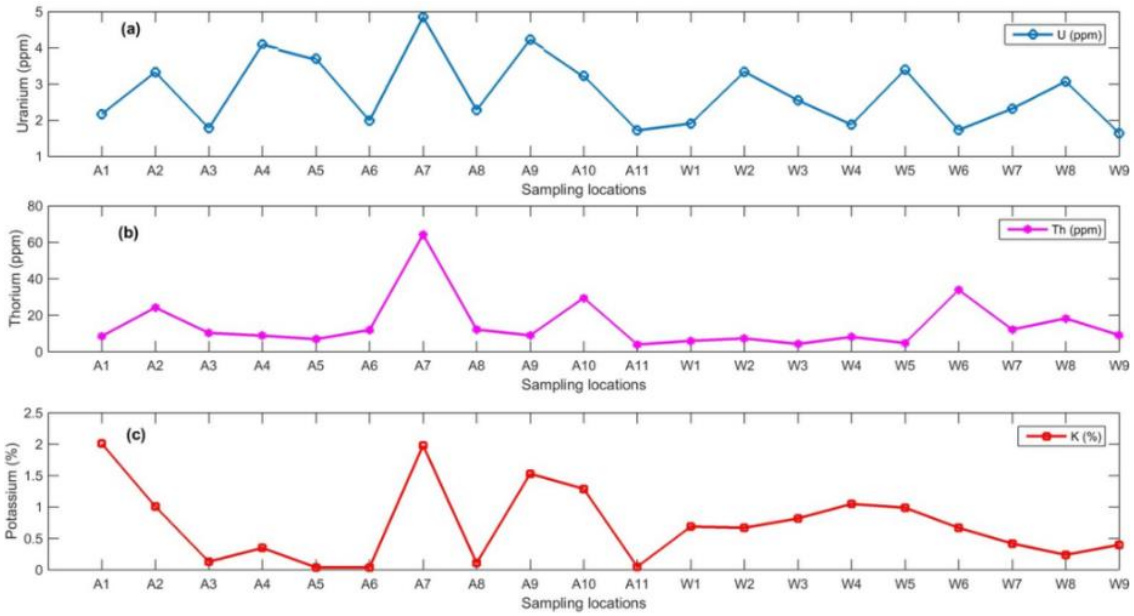

Figure 2: Spectra variation of U- Th- K across the across the lithological units

concentrations of thorium, uranium and potassium in part per million and K (%) is potassium in percentage.

2.6 Uranium Migration Index (UMI)

The Uranium Migration Index (UMI) is a diagnostic tool that reflects the balance between uranium mobility and retention in rocks. UMI is an important factor for environmental risk assessment (since leached uranium may enter groundwater systems), mineralogical exploration and geothermal studies (Youssef et al., 2017). Low UMI indicates good geothermal potential due to retained uranium, high UMI reflects strong weathering and leaching, while very high UMI may point to secondary uranium mineralization prospects. In order to assess the trend of uranium migration in the study area, uranium migration index was calculated using Equation (6) as described by Clarke et al., (1966) and Abuelnaga and Al-Garni, (2015).

$$UMI = eU - \frac{eTh}{3.5} \quad (6)$$

The rate of uranium migration is also a good indicator for determining type and degree of migration. If it is positive; the migration low or moderate, and if it is negative; the migration is high.

3. Results and Discussion

3.1 Spectral U – Th – K trend

The spectral distribution of U, Th and K across the A- and W-transects (A1–A11, W1–W9) reveals significant spatial variability with clear mineralogical and environmental implications (Figure 2 a – c).

Uranium (U) concentrations range between 1.72 (A11) – 4.85 (A7) (2.76) ppm, with prominent anomalies at A4–A5, A7–A9, and moderate values across the W-transect. The result revealed that the uranium concentrations (Figure 2a) present in all the samples were below the world value except nine samples (A2, A4, A5, A7, A9, A10, W2, W5, and W8) which were recorded to have their uranium concentrations above UNSCEAR (2000) world average value of 2.56 ppm.

Thorium (Th) concentrations were found to range between 3.93 (A11) – 64.21 (A7) ppm with average value of 14.67 ppm. Thorium (Th) is generally < 25 ppm but shows a marked peak at A7 (~ 65 ppm) and secondary highs at A2, A9–A11 and W6. Majority of the soil samples were also recorded to have their thorium concentrations above UNSCEAR (2000) world average value of 7.4 ppm. Having the maximum thorium concentration observed in A7 of value 64. 21 ppm (Figure 2b). A7 is found to be from Abeokuta formation all which consists of sandstone, clay and shale. The thorium anomalous levels in those areas may be attributed to the bedrock composition at the sampling points.

Potassium (K) varies between 0.04 (A4, A5) – 2.01 (A1) (0.72) %, with elevated levels at A1, A7, A9–A10 and moderate enrichment in W2–W5. The potassium concentration (Figure 2c) was found to have three of the soil samples, namely; A1, A7 and A9 of the value 2.01, 1.98 and 1.53 % respectively above the average world value 1.3 %.

The strongest multi-element anomaly occurs at A7, where concurrent maxima of U, Th and K indicate a felsic/pegmatitic lithology enriched in K-feldspar, micas, and accessory Th- and U-bearing minerals (monazite, zircon, uraninite). Th-dominant sites (A9–A11, A2) suggest concentration of refractory accessory phases, while isolated U highs with low Th and K (A5 and some W-sites) imply secondary uranium mobility by weathering or hydrothermal transport. K-rich but U-Th poor sites (A1, A9–A10) reflect K-feldspar/mica-rich lithologies with limited radioactive enrichment

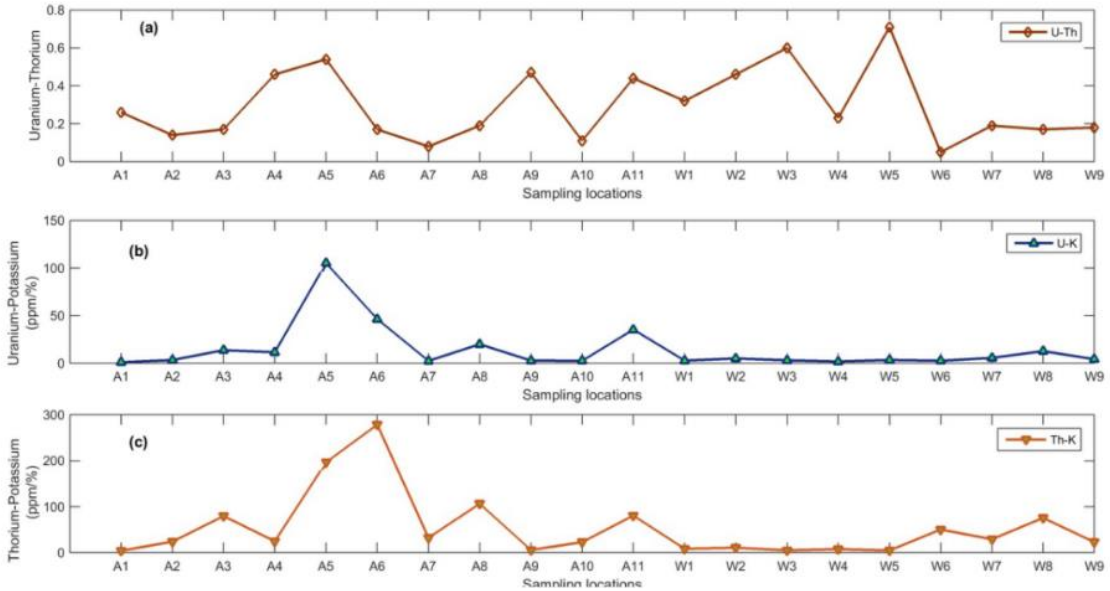

Figure 3: Spectra variation of radioelement ratio U/K U/Th and Th/K across the lithological units

Mineralogically, the A-transect shows greater heterogeneity than the W-transect, suggesting a more complex lithological and alteration history. According to Carvalho et al.(2011), heavy minerals tend to incorporate high concentrations of naturally occurring radionuclides such as eU (ppm) and eTh (ppm) decay series in their crystal structure. They also stated that light minerals such as quartz and feldspar may contain relatively high concentrations of K (%). The gamma ray spectrometric response of rocks and soils varies with the climate to which the area surveyed has been subjected. This is because the response due to fresh bedrock, weathered rocks and transported material differ.

From an environmental perspective, U- and Th-rich zones may pose radiological hazards via enhanced gamma dose rates and radon emanation, while evidence of U mobility highlights the need for groundwater quality assessment.

3.2 Spectral Variation of Radioelement Ratios (U/Th, U/K and Th/K)

The spectral variation of the radioelement ratios U/Th, U/K and Th/K across the studied sampling locations (A1–A11 and W1–W9) reveals significant geochemical and mineralogical insights into the distribution, mobility, and association of uranium, thorium, and potassium within the terrain (Figure 3).

The U/Th ratio (Figure 3a) generally fluctuates between 0.1 and 0.7 across most sampling points, with notable peaks at locations A5, A9, W3 and W5. Elevated U/Th values suggest selective enrichment of uranium relative to thorium, reflecting uranium mobilization under oxidizing conditions and possible secondary deposition in alteration zones. By contrast, low ratios (A6, A10, W6 – W8) indicate uranium depletion or strong thorium dominance, consistent with stable geochemical conditions where uranium remains immobile. From a mineralogical perspective, higher U/Th ratios point to the presence of secondary uranium-bearing minerals such as uranophane, while lower values indicate persistence of resistant thorium minerals like monazite or thorite.

The U/K ratio (Figure 3b) displays highly variable spectral patterns with distinct spikes at A5 and A11, where the ratio exceeds 100 ppm/%. Such anomalies reflect significant uranium enrichment relative to K-bearing minerals. Since potassium is a major constituent of feldspars and micas, elevated U/K values suggest uranium concentration independent of primary silicate minerals, possibly due to hydrothermal alteration or fluid-mediated transport. Lower values, observed in most of the W1–W9 sampling sites, signify uranium retention within K-rich lithologies or absence of notable uranium enrichment. Mineralogically, these anomalies may indicate uraniferous vein-type mineralization superimposed on K-bearing host rocks, while subdued U/K signatures point to unaltered feldspar- or mica-rich lithologies.

The Th/K ratio (Figure 3c) is characterized by pronounced variability, with maximum values (> 250 ppm/%) at A5 and A6, followed by secondary peaks at A3 and A8. These high Th/K ratios suggest thorium enrichment relative to potassium-bearing phases, implying concentration of resistant Th-bearing accessory minerals such as monazite, zircon, or thorite within the host rocks.

Low Th/K values across many western locations (W1–W9) reflect potassium dominance, typical of feldspathic or micaceous lithologies with limited

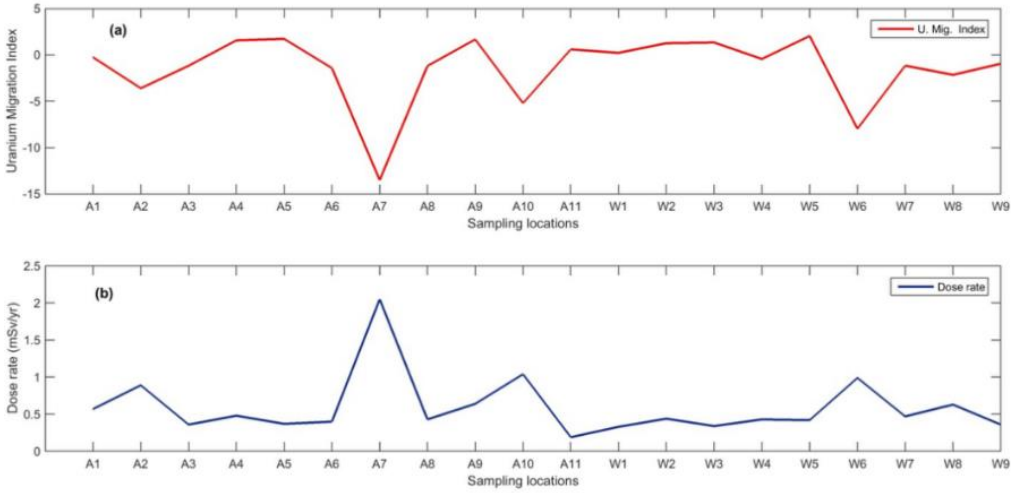

Figure 4: Spectra variation of UMI and Dose rate across the lithological units

thorium mineralization. The spectral pattern, therefore, indicates lithological heterogeneity, where K-rich granitoids coexist with Th-enriched accessory phases in schists and migmatitic host rocks.

The spectral variations highlight zones of uranium mobilization and potential mineralization (A5, A11), thorium enrichment zones dominated by resistant accessory phases (A6, A8), and stable potassium-bearing host lithologies in the western transect. These findings not only elucidate the geochemical behaviour of U, Th, and K but also provide mineralogical evidence essential for both exploration targeting and environmental monitoring.

3.3 Spectral behaviour of the uranium–migration index (UMI) and effective dose rate

The paired spectra show two complementary views of the radiometric regime across the A- and W-transects. Figure 4a depicts the uranium-migration index (UMI) which reflects the relative behaviour of U compared with Th, and Figure 4b accounted for the calculated effective (external) dose rate. Together they discriminate between zones of elemental mobility and zones that dominate the radiological burden.

The UMI curve fluctuates around zero with pronounced excursions: modest positive values at several A-sites (A3–A5) and W-sites, and a very strong negative excursion at A7. The dose-rate spectrum is generally low–moderate (< 1.0 mSv yr^{-1}) over most stations but shows a clear maximum at A7 (the largest peak) and smaller peaks at a few other locations (A10, W5–W7). Notably, the largest negative UMI (A7) coincides with the largest dose-rate peak. In Figure 4, it was observed that only two samples (A7 and A10) have its dose equivalent value to be above 1 mSv/yr. All other soil samples were found to have their dose equivalent value below the UNSCEAR (2000) recommended limit.

High (positive) UMI indicates uranium enrichment relative to thorium (suggesting uranium mobility and secondary concentration), whereas low or negative UMI indicates uranium depletion relative to thorium (either uranium loss or thorium enrichment). The dose rate, in contrast, is driven by the absolute activity of all radioelements (U, Th and K) and thus reports the radiological burden rather than mobility processes.

The coincidence of a very low UMI and a very high dose at A7 implies that the radiological high observed there is not driven by mobile uranium but by large thorium (and/or potassium) activity. This is consistent with the earlier elemental spectra for A7 (very high Th, high K and only moderate U). The Th-dominated sites produce high gamma dose even when U/Th is low. Conversely, locations with positive UMI and modest dose suggest uranium has been relatively enriched compared with Th (possible secondary U concentration) but total activity remains moderate because Th and/or K are low.

Positive UMI anomalies mark potential zones of uranium remobilization and secondary deposition and are valuable vectors for prospecting. Negative UMI where dose is high reflects Th-rich lithologies or felsic differentiation rather than uranium mineralization. High dose-rate stations (A7) require radiological follow-up (site dose confirmation, indoor radon potential, and public exposure assessment) irrespective of UMI sign, because absolute activity controls hazard. Hydrogeologically, the positive UMI values warrant targeted hydrochemical sampling (U concentration and speciation) to check for groundwater contamination pathways; low UMI with elevated dose points more to solid-phase Th hosts and lower short-term mobility risk for dissolved U.

3.4 Spatial Distribution of Radioelements (U-Th-K)

The spatial distribution of radioelements (U, Th, K) and their ratios, provide complementary insights into the geology, mineralization, and environmental risks of the study area. The spatial distribution of the three major radioelements—uranium (U), thorium (Th), and potassium (K) as presented in Figure 5 (a, b, and, c), provides important insights into the lithological framework and geochemical behavior of the study area.

The radiometric data sets were prepared and represented as a contour map for determination of possible radioactive anomaly in the distribution of the radioelements with blue colour denoting low concentrations, green signifies moderate concentration, yellowish-brown represents relative high concentration and pink denotes very high concentration.

Uranium concentrations (Figure 5a) occur as localized anomalies with enrichment most pronounced in the central and southeastern portions of the map. The eU distribution map has eU concentration ranging from 1.260 to 4.085 ppm. For this interpretation, the eU concentration in the study area will be relatively grouped as high (> 4.085 ppm), moderately high (2.261–4.085 pm), moderately low (1.260 – 2.261ppm), and low (< 1.260).

Uranium values are indicators for radioactive mineralization zones. It was found to be more prevalence around the Southern part depicting the presence of limestone with subordinate thinly banded shale, marl and sand in the study area. These zones are characterized by red to pink color anomalies, suggesting possible uranium mineralization or remobilization. In contrast, the northwestern and southwestern zones record relatively low uranium levels, reflecting geologically stable terrains with limited remobilization. The observed enrichment patterns highlight the mobility of uranium under oxidizing conditions, where it may be leached and subsequently reprecipitated along structural or lithological traps.

The eTh map (Figure 5b) displayed the concentration values of the eTh varies from 1.253 to 40.888 ppm.. Low thorium concentration (blue colour) trends from NE part and invariably around SW region. Thorium distribution (Figure 5b) is more widespread and stable compared to uranium.

High Th values are concentrated in the central trending to the southern portions of the area, reflecting the presence of Th-bearing accessory minerals. These minerals are relatively immobile during weathering and hydrothermal alteration, indicating that thorium anomalies are more reflective of primary lithological controls rather than secondary processes.

Potassium distribution (Figure 5c) exhibits distinct enrichment in the central and eastern regions, corresponding to felsic lithologies or zones of potassic alteration. In contrast, southwestern margins are characterized by lower potassium concentrations, which may indicate mafic or altered rock units. The concentration of radioactive potassium (40K) ranges from 0.010 to 1.292%. The strong spatial variability of potassium underscores its role as both a lithological marker and an indicator of hydrothermal alteration processes.

Uranium (U), thorium (Th), and potassium (K) show heterogeneous spatial distributions, with U and Th exhibiting localized highs in the central and northeastern zones. Potassium is more broadly distributed, reflecting its abundance in feldspar-rich lithologies. The clustering of high U and Th suggests localized mineralization and lithological controls, possibly linked to felsic intrusions or vein-related deposits.

3.5 Spatial Distribution of Radioelements Ratios (U/K, U/Th and Th/K)

The radioelement ratio maps (Figure 6a–c) further refine the interpretation by normalizing elemental abundances against one another, thereby emphasizing relative enrichments and depletion trends. The U/K ratio (Figure 6a) displays strong anomalies in the central and southeastern zones, suggesting selective uranium enrichment relative to potassium. This pattern is often diagnostic of hydrothermal leaching and redeposition of uranium, particularly in terrains with structurally controlled fluid pathways.

The U/K ratio captures uranium behavior relative to stable K-bearing minerals such as feldspars and micas. High values signify uranium enrichment due to hydrothermal activity, weathering, or migration, while low values indicate uranium depletion or K-enrichment, often linked to potassic alteration. This makes the U/K ratio particularly effective in identifying alteration halos and leached zones.

The U/Th ratio (Figure 6b) is generally low across the study area, reflecting the relative immobility of thorium. However, localized high U/Th anomalies occur in the central sector, marking areas of potential secondary uranium enrichment where uranium has been mobilized and concentrated relative to thorium. The U/Th ratio reflects the relative mobility of uranium, with elevated values indicating enrichment through mobilization and secondary deposition under oxidizing conditions, whereas low ratios suggest uranium depletion or retention within resistant minerals. Anomalous U/Th zones are therefore often linked to secondary uranium mineralization or hydrothermal alteration.

Finally, the Th/K ratio (Figure 6c) highlights lithological contrasts, with high values concentrated in the northern and southwestern portions of the study area. These anomalies suggest terrains dominated by Th-bearing resistant minerals relative to K-feldspar–

rich rocks. Conversely, lower Th/K values correspond to K-enriched zones, which may represent feldspathic lithologies or potassic alteration halos associated with magmatic or hydrothermal processes. The Th/K ratio, largely controlled by immobile mineral phases, serves as a lithological discriminator. High ratios indicate thorium enrichment in resistant accessory minerals typical of felsic igneous rocks, while low values may reflect K-enrichment or thorium loss during weathering.

High U/K and U/Th zones mark areas of uranium enrichment relative to K and Th, suggesting mobilization and possible secondary uranium concentration. Conversely, low U/Th ratios imply uranium depletion through leaching, leaving behind thorium-rich residues. The Th/K map highlights zones of felsic–mafic lithological contrast, useful for delineating basement rock boundaries.
The combined use of elemental distributions and ratio maps provides a robust framework for understanding both the lithological controls and secondary geochemical processes operating in the study area. Uranium exhibits strong mobility, with its enrichment largely restricted to structurally favorable zones, while thorium anomalies provide reliable markers of primary lithologies.

Potassium distribution reflects both lithological variation and alteration effects, reinforcing its value in delineating felsic intrusions and hydrothermal systems. The ratio maps (U/K, U/Th, Th/K) enhance anomaly contrast and discrimination, allowing for the identification of zones where secondary uranium mineralization may have occurred and distinguishing these from background lithological variations. This integrative approach underscores the importance of coupling radioelement concentration data with ratio analyses to guide exploration strategies for uranium and related mineral resources.

Carvalho et al. (2011), realized that high values of eTh/K are characterized by the presence of heavy minerals and also low values of eTh/K are characterized by the presence of light minerals However, in Figure 6, it was observed that the Th/K values are higher (above 0.5) across all the formations. From the result obtained, it can be recognized that eTh on the southwestern part of the map comparing with potassium percentage is much larger. High Th/K ratios (Figure 5) are linked with clay-mineral suites dominated by kaolinite, whereas low Th/K ratios are associated with clay-mineral assemblages dominated by mixed-layer clays. The overall field possessed more kaolinite and chlorite, as seen by the variation of Th/K ratios (Figure 5).

These ratios are invaluable for mineralogical assessment, alteration mapping, and exploration targeting. Elevated U/Th and U/K values delineate potential uranium mobilization zones and alteration halos, whereas Th/K aids in differentiating felsic from mafic lithologies and identifying areas of potassic alteration. Beyond exploration, these ratios also provide environmental insights, helping to track uranium mobilization, assess weathering intensity, and pinpoint contamination hotspots.

3.6 Dose Rate and Uranium Migration Index

The spatial dose rate map (Figure 7a) reveals values ranging from 0.172 to 1.253 mSv/yr. High dose zones (pink to red) with values (> 1.0 mSv/yr) are concentrated in the central and north-eastern portions of the survey area. These coincide with high U and Th concentrations, as observed in the radioelement maps (Figure 5). Moderate zones (green to yellow) dominate the central portions, while low dose zones (blue shades) with background levels (< 0.48 mSv/yr) dominate the western margins, indicating relatively low radioelement content. This high dose observed exceed the ICRP's recommended annual limit for public exposure, highlighting localized radiation hotspots with potential health risks.
The uranium migration index (UMI) map (Figure 7b) ranges from –9.256 to +4.580, reflecting contrasting uranium stability across the terrain. Negative values correspond to stable lithologies where uranium remains fixed within host rocks, while positive values delineate areas of active leaching and redistribution. Notably, high UMI zones in the northeastern and southeastern portions overlap with elevated dose rates, indicating both heightened environmental risk and potential secondary uranium enrichment.

Uranium exhibits greater mobility than thorium and potassium in surface and near-surface environments, particularly under oxidizing conditions. The Uranium Migration Index (UMI) provides a measure of this mobility, quantifying the degree to which uranium has been leached, redistributed, or retained relative to more immobile elements. Low UMI values indicate that uranium remains bound within its host rock, whereas high values reflect significant mobilization and secondary accumulation.

In this study, low to moderate UMI values are environmentally and energetically favorable, as uranium retention ensures sustained radiogenic heating and lithological stability—key factors for geothermal resource potential. By contrast, high UMI values point to zones of strong weathering and alteration, where uranium has been leached from the primary rock mass. Such areas display reduced geothermal capacity but may represent targets for secondary uranium mineralization, particularly in roll-front or depositional settings. The UMI interpretation distinguishes between stable, heat-producing lithologies suitable for geothermal exploitation and altered zones that, while less favorable for long-term energy generation, may carry economic significance for uranium exploration.

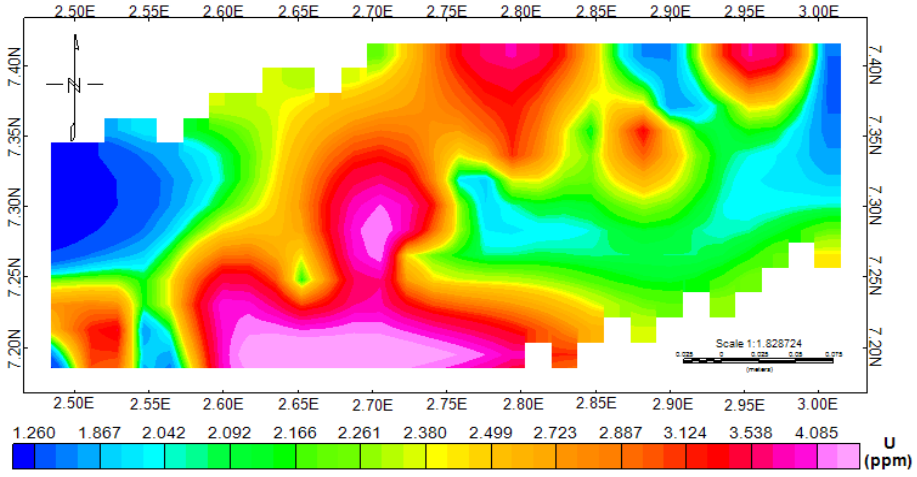

(a)

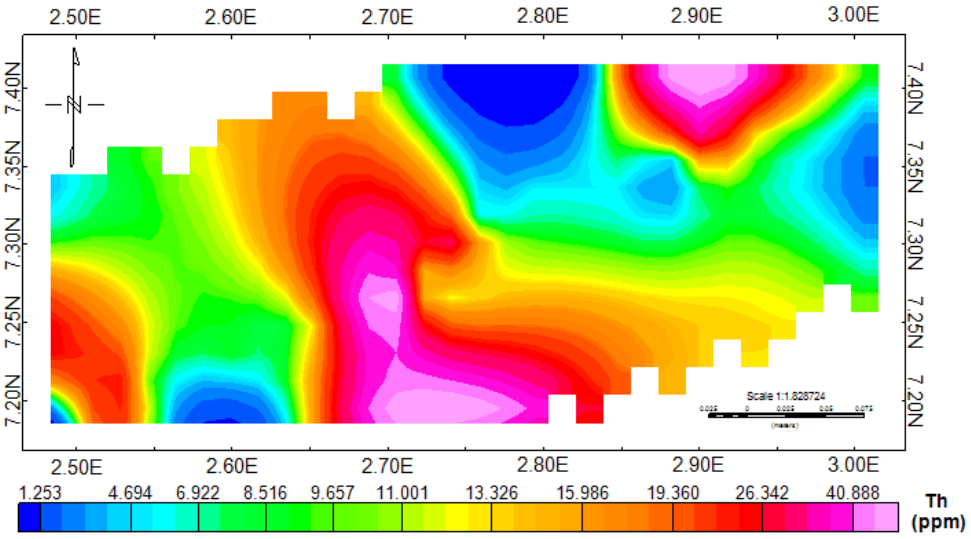

(b)

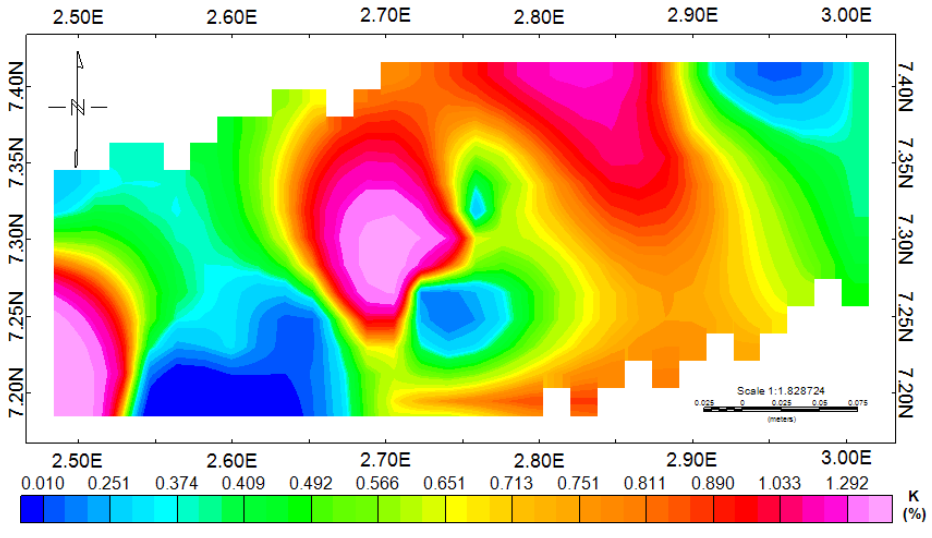

(c)

Figure 5: Spatial radioelements contour map of (a) Uranium (b) Thorium (c) Potassium

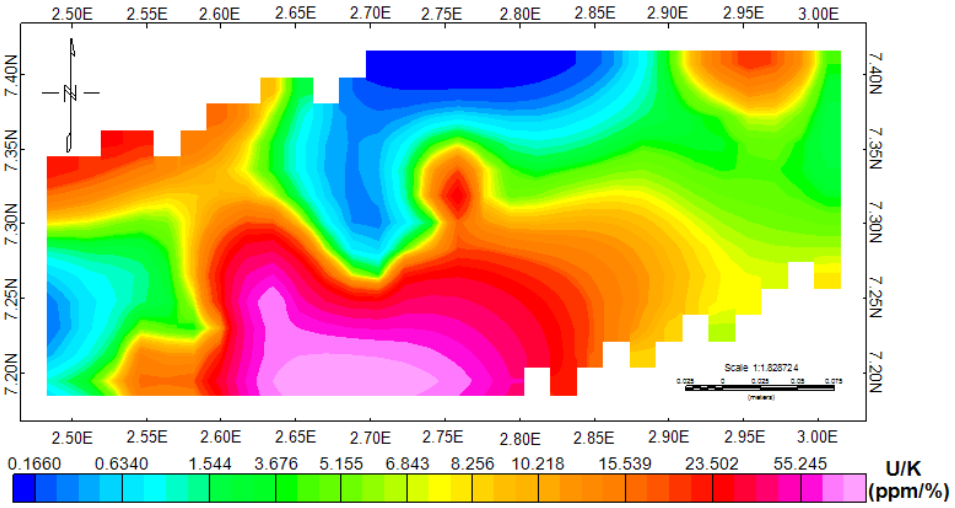

(a)

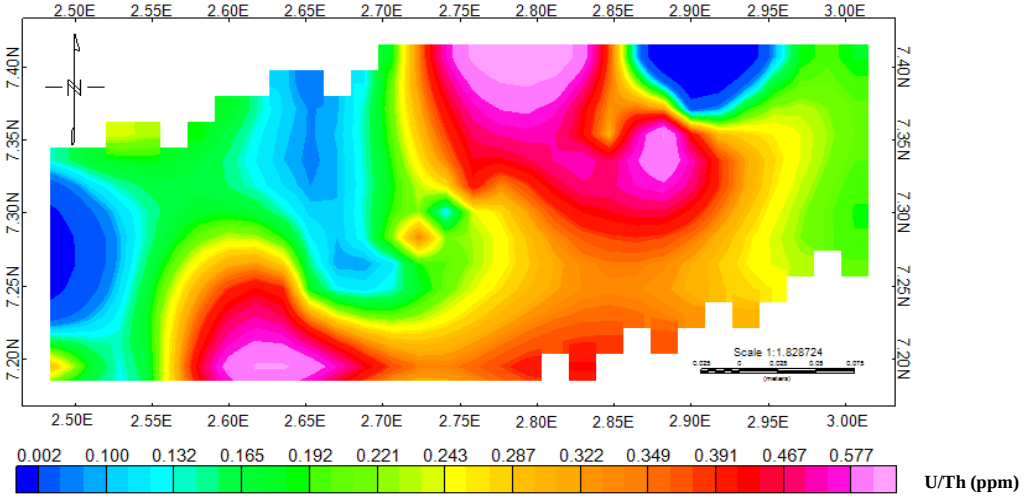

(b)

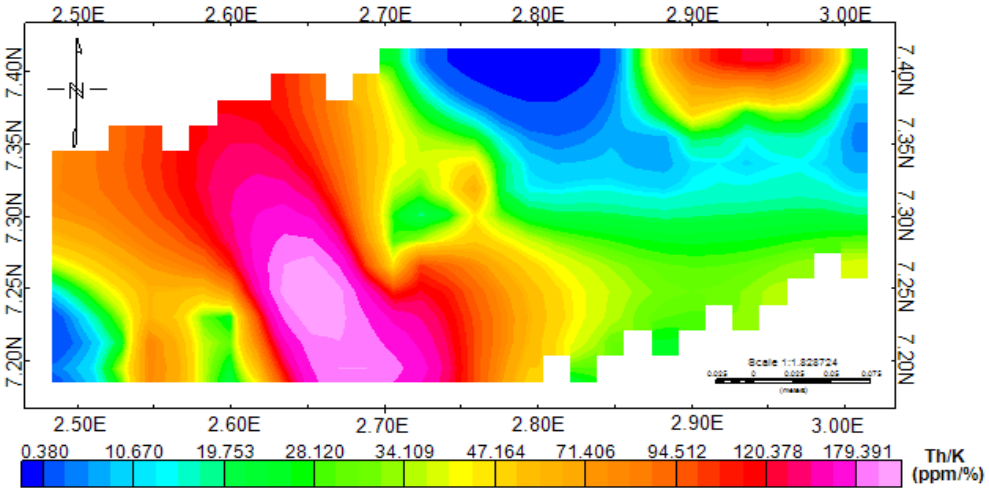

(c)

Figure 6: Spatial radioelements ratio contour map of (a) U/K (b) U/Th (c) Th/K

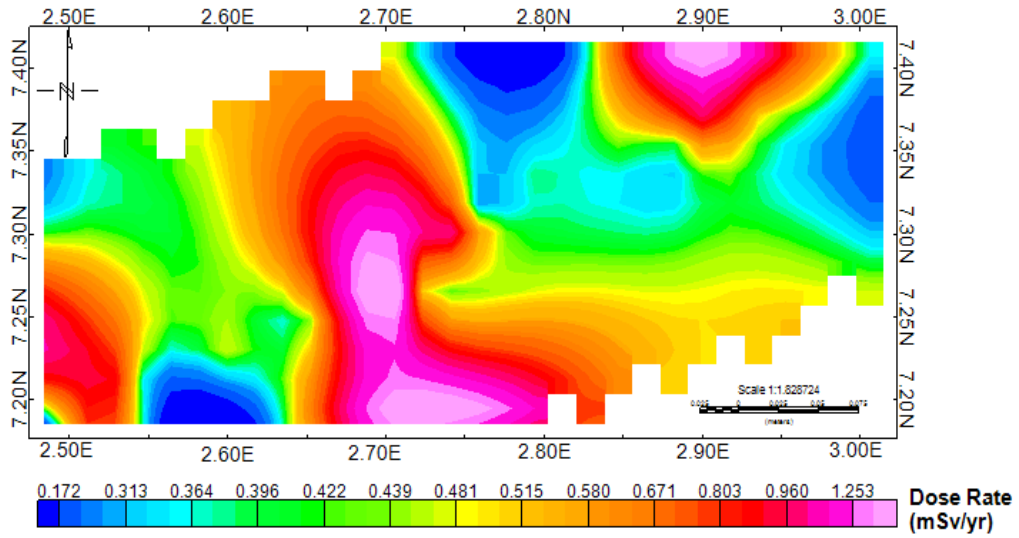

(a)

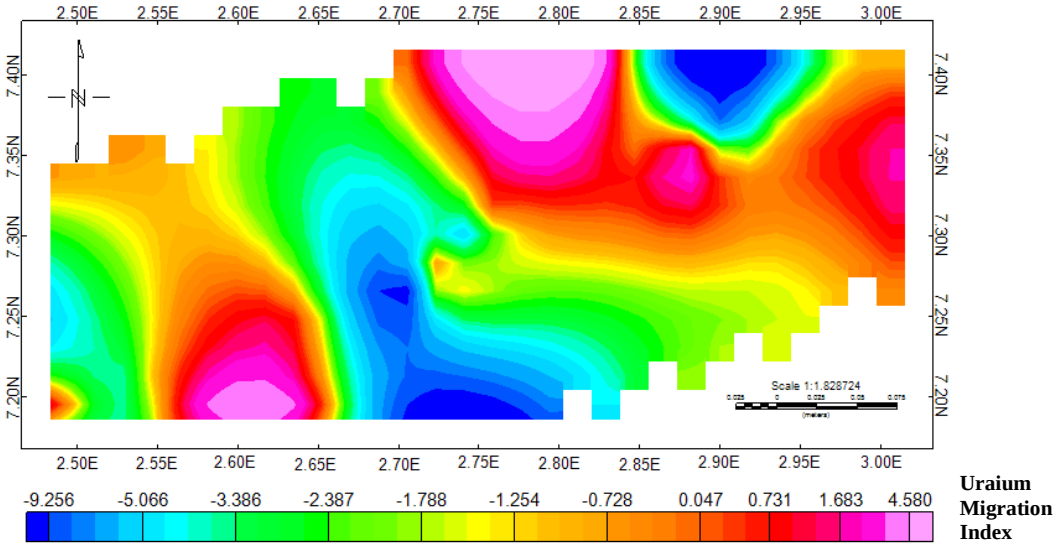

(b)

Figure 7: Spatial contour map of (a) Dose rate (b) Uranium Migration Index

Elevated dose rate zones exceeding 1.0 mSv/yr present potential long-term health risks, including increased cancer incidence and genetic effects, while uranium decay may also enhance indoor radon exposure in nearby communities. Positive UMI zones further highlight areas of uranium mobilization, where soluble U^{6+} can contaminate groundwater systems (Ademoroti *et al.*, 2024; Mbonu *et al.*, 2025). Prolonged ingestion of uranium-rich water is linked to kidney toxicity and skeletal accumulation, underscoring the need for hydrogeological monitoring.

Beyond radiological hazards, uranium and its decay products may enter the soil–plant system in mobilization zones, leading to bioaccumulation in crops and extending exposure pathways to humans and animals. Environmentally, these areas demand careful land-use planning, while geologically, they mark potential sites of secondary uranium enrichment. By contrast, negative UMI zones represent stable host rocks with minimal uranium leaching, posing lower environmental risks but offering limited exploration potential.

Together, these results underscore dual implications: (i) environmental and health concerns, where radiation exposure and groundwater contamination risks are highest in positive UMI zones; and (ii) exploration significance, as areas of uranium mobilization mark potential sites for secondary mineralization. Thus, the integrated use of dose rate and UMI maps provides a robust framework for both radiological hazard assessment and resource evaluation.

4. Conclusion

The study area is characterized by heterogeneous radioelement distribution, structurally guided uranium mobilization, and localized radiation hotspots. These findings have significant implications for both uranium exploration and environmental health monitoring, necessitating integrated geological, geochemical, and radiological assessments.

The spatial coincidence of high U/Th ratios, elevated dose rates, and positive UMI highlights structurally controlled pathways such as faults or shear zones that facilitated uranium mobilization. These structures represent both environmental vulnerabilities and exploration targets for secondary uranium deposits.

The integration of these datasets reveals that uranium-rich zones not only pose radiation hazards but also represent areas of active uranium migration. This dual significance underscores the importance of monitoring groundwater quality in positive UMI regions, as uranium can dissolve under oxidizing conditions, contaminating aquifers and impacting public health. Agriculturally, radionuclide uptake by crops in these zones could introduce additional exposure pathways.

References

Abdel-Hakeem, M., El-Tahir, M., Zeid, E. A., & Rageh, H. (2023). Genetic implications of Th/U, Th/K, and U/K ratios for uranium mineralizations: A case study from El-Missikat and El-Erediya shear zones, Eastern Desert, Egypt. Geochemical Transactions, 24(3), 1–18.

Abuelnaga, H. S. O., & Al-Garni, M. A. (2015). Airborne gamma-ray spectrometric and magnetic studies of Wadi Um Geheig–Wadi Abu Eligam area, Central Eastern Desert, Egypt. Arabian Journal of Geosciences, 8(10), 8811–8833.

Abu-Khader, M. M., Shawaqfeh, A. T., Naddaf, Z., Maity, J. P., & Bhattacharya, P. (2018). Radon in the groundwater in the Amman-Zarqa Basin and related environments in Jordan. Groundwater for Sustainable Development, 7, 73–81.

Ademila, O., Akingboye, A. S., & Ojamomi, A. I. (2023). Radiometric survey in geological mapping of parts of basement complex area of Nigeria. Vietnam Journal of Earth Sciences, 40(3), 306–319.

Ademoroti, A., et al. (2024). Radiometric survey of background ionizing radiation and assessment of radiological health risk on the residents of Agbarho Kingdom, Delta State, Nigeria. Nigerian Journal of Physics, 32(3), 45–56.

Akingboye, A. S., Ademila, O., Okpoli, C. C., Oyeshomo, A. V., Ijaleye, R. O., Faruwa, A. R., Adeola, A. O., & Bery, A. A. (2022). Radiogeochemistry, uranium migration, and radiogenic heat of the granite gneisses in parts of the southwestern Basement Complex of Nigeria. Journal of African Earth Sciences, 188, 104469.

Altundaş, S. (2021). Uranium migration and radioactive characteristics of the Saricicek and Sarihan granodiorites and surroundings. Turkish Journal of Engineering, 5(2), 82–90.

Altundaş, S., & Çınar, H. (2023). Uranium migration and radioactive characteristics of the Sarıçiçek and Sarıhan granodiorites. Turkish Journal of Engineering, 7(3), 208–226.

Asfahani, J., Aissa, M., & Al-Hent, R. (2007). Uranium migration in sedimentological phosphatic environment in Northern Palmyrides, Al-Awabed Area, Syria. Applied Radiation and Isotopes, 65(10), 1078–1086.

Bayoumi, M. B., & Emad, B. M. (2020). Mapping and lithological discrimination using digital image processing and radioactive investigations of Wadi Um Gheig area, Central Eastern Desert, Egypt. Middle East Journal of Applied Sciences, 10(4), 737–754.

Carvalho, C. Anjos R.M., Veiga R, & Macario K. (2011). Application of radiometric analysis in the study of provenance and transport processes of Brazilian coastal sediments, J. Environ. Radioact. 102 185–192.

Clark, S. P., Peterman, Z. E., & Heier, K. S. (1966). Abundance of U, Th, and K. In S. P. Clark (Ed.), Handbook of physical constants (Vol. 97, pp. 521–541). Geological Society of America.

Dabayneh, K. M., Mashal, L. A., & Hasan, F. I. (2008). Radioactivity concentration in soil samples in the southern part of the West Bank, Palestine. Radiation Protection Dosimetry, 131(2), 265–271.

Eke, B. C., Akomolafe, I. R., Ukewuihe, U. M., & Onyenegecha, C. P. (2024). Assessment of radiation hazard indices due to natural radionuclides in soil samples from Imo State University, Owerri, Nigeria. Environmental Health Insights, 18, 1–12.

Elegbede, A. J., Bogun, F. J., Dare, S. O., & Leebana, E. A. (2025). Elevated natural radionuclides in soils and stream sediments: Pollution, spatial distribution, radiological hazards, and cancer risks in peri-urban Emure-Ekiti, southwest Nigeria. Discover Soil. Advance online publication.

El-Qassas, R. A. Y. (2020). Airborne gamma-ray spectrometric data interpretation for uranium exploration: eU/eTh ratio mapping and favorability indices. Journal of Applied Geophysics, 176, 104–115.

Faweya, E. B., & Babalola, A. I. (2010). Radiological safety assessment and occurrence of heavy metals in soil from designated waste dumpsites used for building and compositing in southwestern Nigeria. Arabian Journal for Science and Engineering, 35(2A), 219–225.

Hennig, T. & Kühn, M. (2021). Potential uranium migration within the geochemical gradient of the Opalinus Clay system at the Mont Terri. Minerals, 11(10), 1087.

International Atomic Energy Agency (IAEA) (2003). Guidelines for radioelement mapping using gamma ray spectrometry data. TECHREPORT 1363, Vienna, Austria, p. 14.

ICRP (1994). *ICRP Publication 65: Protection Against Radon-222 at Home and at Work* (SAGE Publications, 1994).

Khattab, M. R., Tawfic, A. F., & Omar, A. M. (2021). Uranium-series disequilibrium as a tool for tracing uranium accumulation zone in altered granite rocks. International Journal of Environmental Analytical Chemistry, 101(12), 1750–1760.

Makinde, O. W., Ogundele, K. T., & Tubosun, I. A. (2023). Radionuclide concentration of soil and sediment in gold-mining locations of Atakumosa-West Local Government, South-West, Nigeria. International Journal of Environmental Monitoring and Analysis, 11(3), 57–62.

Malczewski, D., Teper, L., & Dorda, J. (2004). Radioactivity of selected rocks and natural radiation in the environment of the Sudetes, southwestern Poland. Journal of Environmental Radioactivity, 75(3), 193–209.

Mbonu, C. C., Agbalagba, E. O., Mbonu, J. E., Ben, U. C., Mbonu, I. J., Abdelrahman, K., Fnais, M. S., Gomez-Ortiz, D., Agiande, D., & Eldosouky, A. M. (2025). Assessment of terrestrial radionuclide exposure and contamination rates within the Mbaitoli area, Nigeria. Scientific Reports, 15(1), 28702.

Ogunsanwo**,** F.O, Ayanda**,** J.D, Mustapha**,** A.O, Olatunji**,** A.T, Ozebo**,** V.C, Olurin**,** O.T, Alaka, A.O, Okeyode**,** I.C, Adepitan**,** J.O & Olowofela, J.A. (2023). Empirical Relation between Magnetic and Radiometric Survey in Bitumen Area, Ogun State, Nigeria. *Materials and Geoenvironment*, 69(2): 1-14. .

Ogunsanwo, F.O, Mustapha, A.O, Ozebo, V.C, Okeyode, I.C, Ayanda, J.D & Sanni, K.R. (2025). Empirical and spatial relation between magnetic and radiometric survey over mica schist area, Ogun State, Nigeria. *FUDMA Journal of Sciences, 9(9), 287 – 297.*

Okoro, L. O., Ugwu, G. Z., & Onyishi, G. E. (2023). Interpretation of high-resolution airborne radiometric data over part of Lower Benue Trough, Nigeria. African Journal of Environment and Natural Science Research, 6(3), 132–142.

Olawale, I. A., Ojo, F. M., & Karigidi, K. O. (2024). Radiometric investigation of naturally occurring radionuclides in soils from Igbokoda, a coastal area in Ondo State, Nigeria. Journal of the Nigerian Society of Physical Sciences, 6(4), 1–12.

Olowofela, J. A., Okeyode, I. C., Idowu, O. A., Olurin, O. T., & Ogunsanwo, F. O. (2019). Lithological mapping of Ogun State, Southwestern Nigeria, using aeroradiospectrometry. Environmental Earth Sciences, 78(7): 263.

Pujol, L., & Sánchez-Cabeza, J. A. (2000). Natural and artificial radioactivity in surface waters of the Ebro River basin (Spain). Journal of Environmental Radioactivity, 51(2), 181–210.

UNSCEAR. (2000). Sources and effects of ionizing radiation (Vol. I: Sources; Vol. II: Effects). United Nations Scientific Committee on the Effects of Atomic Radiation, Report to the General Assembly, with scientific annexes. United Nations.

Uwah, E. J., & Rosenberg, R. J. (1993). Measurement of radioelement contents of rocks of Ugep, Southeastern Nigeria, by gamma-ray spectrometric and instrumental neutron activation analysis techniques. Applied Radiation and Isotopes, 44(5), 855–858.

Uyanık, N. A. (2022). Determination of alteration zones and geological unit limits using airborne radiometric properties — case study. Applied Radiation and Isotopes / Journal of Geophysics.

Youssef, M. A. S., Sabra, M. E. M., Abdeldayem, A. L., Masoud, A. A., & Mansour, S. A. (2017). Uranium migration and favourable sites of potential radioelement concentrations in Gabal Umm Hammad area, Central Eastern Desert, Egypt. NRIAG Journal of Astronomy and Geophysics, 6(2), 328–339.